Monolithic dual-mode distributed feedback semiconductor laser for tunable continuous-wave terahertz generation

Namje Kim[1], Jaeheon Shin[1], Eundeok Sim[1], Chul Wook Lee[1], Dae-Su Yee[2], Min Yong Jeon[3], Yudong Jang[2], and Kyung Hyun Park[1,*]

[1]Photonic/Wireless Convergence Components Department, ETRI, Daejeon 305-700, Korea
[2]Center for Safety Measurement, KRISS, Daejeon 305-340, Korea
[3]Department of Physics, Chungnam National University, Daejeon 305-764, Korea,
** khp@etri.re.kr, myjeon@cnu.ac.kr*

Abstract: We report on a monolithic dual-mode semiconductor laser operating in the 1550-nm range as a compact optical beat source for tunable continuous-wave (CW) terahertz (THz) generation. It consists of two distributed feedback (DFB) laser sections and one phase section between them. Each wavelength of the two modes can be independently tuned by adjusting currents in micro-heaters which are fabricated on the top of the each DFB section. The continuous tuning of the CW THz emission from Fe^+-implanted InGaAs photomixers is successfully demonstrated using our dual-mode laser as the excitation source. The CW THz frequency is continuously tuned from 0.17 to 0.49 THz.

OCIS codes: (140.5960) Semiconductor lasers; (140.3600) Lasers, tunable; (300.6495) Spectroscopy, terahertz

References and links

1. M. Tonouchi, "Cutting-edge terahertz technology," Nat. Photonics **1**(2), 97–105 (2007).
2. I. Hosako, N. Sekine, M. Patrashin, S. Saito, K. Fukunaga, Y. Kasai, P. Baron, T. Seta, J. Mendrok, S. Ochiai, and H. Yasuda, "At the Dawn of a New Era in Terahertz Technology," Proc. IEEE **95**(8), 1611–1623 (2007).
3. Y. C. Shen, P. C. Upadhya, H. E. Beere, E. H. Linfield, A. G. Davies, I. S. Gregory, C. Baker, W. R. Tribe, and M. J. Evans, "Generation and detection of ultra broadband terahertz radiation using photoconductive emitters and receivers," Appl. Phys. Lett. **77**, 4104 (2004).
4. E. R. Brown, J. R. Soderstrom, C. D. Parker, L. J. Mahoney, K. M. Molvar, and T. C. McGill, "Oscillations up to 712 GHz in InAs/AlSb resonant-tunneling diodes," Appl. Phys. Lett. **58**(20), 2291 (1991).
5. M. A. Belkin, F. Capasso, F. Xie, A. Belyanin, M. Fischer, A. Wittmann, and J. Faist, "Room temperature terahertz quantum cascade laser source based on intracavity difference-frequency generation," Appl. Phys. Lett. **92**(20), 201101 (2008).
6. I. S. Gregory, C. Baker, W. R. Tribe, I. V. Bradley, M. J. Evans, E. H. Linfield, A. G. Davies, and M. Missous, "Optimization of photomixers and antennas for continuous-wave terahertz emission," IEEE J. Quantum Electron. **41**(5), 717–728 (2005).
7. H. Ito, F. Nakajima, T. Furuta, and T. Ishibashi, "Continuous THz-wave generation using antenna-integrated uni-travelling-carrier photodiodes," Semicond. Sci. Technol. **20**(7), S191–S198 (2005).
8. J. R. Demers, R. T. Logan, Jr., and E. R. Brown, "An Optically Integrated Coherent Frequency-Domain THz Spectrometer with Signal-to-Noise Ratio up to 80 dB," Microwave Photonics Tech. Digest, Victoria, Canada (2007), pp. 92–95.
9. A. Klehr, J. Fricke, A. Knauer, G. Erbert, M. Walther, R. Wilk, M. Mikulics, and M. Koch, "High-power monolithic two-mode DFB laser diode for the generation of THz radiation," IEEE J. Sel. Top. Quantum Electron. **14**(2), 289–294 (2008).
10. P. Gu, M. Tani, M. Hyodo, K. Sakai, and T. Hidaka, "Generation of cw-Terahertz Radiation Using a Two-Longitudinal-Mode Laser Diode," Jpn. J. Appl. Phys. **37**(Part 2, No. 8B), L976–L978 (1998).
11. S. Osborne, S. O'Brien, E. P. O'Reilly, P. G. Huggard, and B. N. Ellison, "Generation of CW 0.5 THz radiation by photomixing the output of a two-colour 1.49 μm Fabry-Perot diode laser," Electron. Lett. **44**(4), 296 (2008).
12. R. Hui, B. Zhu, K. Demarest, C. Allen, and Jin Hong, "Generation of ultrahigh-speed tunable-rate optical pulses using strongly gain-coupled dual-wavelength DFB laser diodes," IEEE Photon. Technol. Lett. **11**(5), 518–520 (1999).

#113331 - $15.00 USD Received 24 Jun 2009; revised 7 Jul 2009; accepted 7 Jul 2009; published 24 Jul 2009

13. R. Phelan, V. Weldon, M. Lynch, and J. F. Donegan, "Simultaneous multigas detection with cascaded strongly gain coupled DFB laser by dual wavelength operation," Electron. Lett. **38**(1), 31 (2002).
14. S. Hoffmann, M. Hofmann, M. Kira, and S. W. Koch, "Two-colour diode lasers for generation of THz radiation," Semicond. Sci. Technol. **20**(7), S205–S210 (2005).
15. S. Pajarola, G. Guekos, and J. Mork, "Optical Generation of Millimeter-Waves Using a Dual-Polarization Emission External Cavity Diode Laser," IEEE Photon. Technol. Lett. **8**(1), 157–159 (1996).
16. H. Page, S. Malik, M. Evans, I. Gregory, I. Farrer, and D. Ritchie, "Waveguide coupled terahertz photoconductive antennas: Toward integrated photonic terahertz devices," Appl. Phys. Lett. **92**(16), 163502 (2008).
17. K. H. Park, Y. A. Leem, D. S. Yee, Y. Baek, D. C. Kim, S. B. Kim, and E. Sim, "Self-Pulsation in Multisection Distributed Feedback Laser Diode with a Novel Dual Grating Structure," ETRI J. **25**(3), 149–155 (2003).
18. O. Brox, S. Bauer, M. Radziunas, M. Wolfrum, J. Sieber, J. Kreissl, B. Sartorius, and H.-J. Wünsche, "High-Frequency Pulsations in DFB Lasers With Amplified Feedback," IEEE J. Quantum Electron. **39**(11), 1381–1387 (2003).
19. D. S. Yee, Y. A. Leem, S. B. Kim, D. C. Kim, K. H. Park, S. T. Kim, and B. G. Kim, "Loss-coupled distributed-feedback lasers with amplified optical feedback for optical microwave generation," Opt. Lett. **29**(19), 2243–2245 (2004).
20. Y. A. Leem, D. S. Yee, E. Sim, S. B. Kim, D. C. Kim, and K. H. Park, "Self-pulsation in multisection laser diodes with a DFB reflector," IEEE Photon. Technol. Lett. **18**(4), 622–624 (2006).
21. S. Sakano, T. Tsuchiya, M. Suzuki, S. Kitajima, and N. Chinone, "Tunable DFB Laser with a Striped Thin-Film Heater," IEEE Photon. Technol. Lett. **4**(4), 321–323 (1992).
22. S. W. Ryu, S. B. Kim, J. S. Sim, Y. D. Chung, J. H. Lee, and J. Kim, "Monolithic integration of thin film μ-heater array with 4-channel WDM transmitter," Microelectron. J. **35**(2), 203–206 (2004).
23. S. H. Oh, C. W. Lee, J. M. Lee, K. S. Kim, H. Ko, S. Park, and M. H. Park, "The Design and the Fabrication of Monolithically Integrated GaInAsP MQW Laser With Butt-Coupled Waveguide," IEEE Photon. Technol. Lett. **15**(10), 1339–1341 (2003).
24. G. P. Li, T. Makino, R. Moore, N. Puetz, K. Leong, and H. Lu, "Partly Gain-Coupled 1.55 μm Strained-Layer Multiquantum-well DFB Lasers," IEEE J. Quantum Electron. **29**(6), 1736–1742 (1993).
25. B. W. Hakki, and T. Paoli, "Gain spectra in GaAs double heterostructure injection lasers," J. Appl. Phys. **46**(3), 1299 (1975).
26. C. Carmody, H. H. Tan, C. Jagadish, A. Gaarder, and S. Marcinkevičius, "Ion-Implanted InGaAs for ultrafast optoelectronic applications," Appl. Phys. Lett. **82**(22), 3913 (2003).
27. J. Mangeney, A. Merigault, N. Zerounian, P. Crozat, K. Blary, and J. F. Lampin, "Continuous wave terahertz generation up to 2 THz by photomixing on ion-irradiated InGaAs at 1.55 μm wavelengths," Appl. Phys. Lett. **91**(24), 241102 (2007).

1. Introduction

Terahertz (THz) frequency sources have received considerable attention for their medical, agriculture, environmental, and security applications [1,2]. Over the past decades, significant progress has been realized in the field of THz time-domain spectroscopy (TDS) using photoconductive antennas (PCAs) and femtosecond pulsed lasers [3]. The TDS systems, however, have some drawbacks on the field applications because of their size, cost, and power consumption. In many cases of THz applications, the frequency-tunable continuous-wave (CW) operation of the radiation source with compact size and low cost is preferable. Resonant tunneling diodes and quantum cascade lasers (QCLs) have been studied as compact CW THz sources, however, there is a limitation on frequency tunability [4,5]. Furthermore, QCL has a difficulty on room-temperature CW operation. Up to now, the most promising candidate as a portable and widely-tunable CW THz emitter is the combination of a photomixer and an optical beat source [6,7]. The optical beat sources are typically composed of two tunable distributed feedback (DFB) or distributed Bragg reflector (DBR) laser diodes (LDs) having different wavelengths [8]. However, the use of two independent lasers still introduces considerable efforts in stabilizing each frequency and matching the two beams spatially. A remarkable simplification could be achieved by using laser systems that are forced to emit two wavelengths simultaneously.

Various semiconductor dual-mode lasers have been recently studied for the compact and low-cost optical beat source for THz photomixing. They can be classified into three groups. Dual-mode lasers which typically use the frequency selective structures such as phase-shift DBR, and spatially-varying refractive-index profile are categorized into the first group [9–11]. Although those devices show a stable dual-mode operation by two longitudinal modes in

#113331 - $15.00 USD Received 24 Jun 2009; revised 7 Jul 2009; accepted 7 Jul 2009; published 24 Jul 2009

a single cavity, they have a limitation in tuning the mode beat frequency which corresponds to the wavelength difference between two longitudinal modes. Secondly, multisection DFB LDs based on strong gain-coupled grating were also investigated by several research groups [12,13]. However, the tuning ranges were all reported to be very narrow – less than 100 GHz – because of the lack of efficient tuning methods. Finally, broad frequency tuning has been demonstrated by using external-cavity lasers which emit two wavelengths simultaneously [14,15]. However, the external-cavity lasers have disadvantages of the mechanical moving part for wavelength tuning and high cost.

In this paper, we demonstrate a novel monolithic dual-mode DFB laser operating in the 1550-nm range using all-active multisection structure with precise and broad-range wavelength tuning. Each wavelength of the two modes can be independently tuned by adjusting currents in micro-heaters (μ-heaters) which are fabricated on the top of the each DFB section. The continuous frequency tuning of the CW THz emission is also successfully achieved using Fe^{+}-implanted InGaAs photomixers and our dual-mode laser as an excitation source. The use of 1550-nm range dual-mode LD could bring the connection between the THz and InP-based communication technologies since the well-developed InP-based optoelectronic technologies are expected to enable the integration of tunable LD sources with other optical components such as semiconductor optical amplifiers (SOAs), electro-absorption modulators, and waveguide-type THz photomixers [16].

2. Device fabrication

The wavelength-tunable dual-mode LD (DML) is fabricated as shown in Fig. 1. The structure is composed of one phase and two DFB sections. The lengths of the phase and DFB sections are 50 μm and 300 μm, respectively. μ-heaters are used to tune the operating wavelengths of the two laser modes of the DML independently. Monolithic multisection LDs generating mode beating and self-pulsations have been developed in order to use in optical communication systems [17–20]. However, their tuning range and self-pulsation frequency are typically below 100 GHz. Moreover, the injection-current variation for the tuning of beat frequency breaks the power balance between two lasing modes. The easiest and cost effective method to extend the tuning range is to use the integrated μ-heater which has been widely used for continuous wavelength tuning in various devices [21,22]. To independently control each lasing mode, μ-heaters are integrated on top of each DFB-LD section as shown in Fig. 1. And both the device structure and the shape of the μ-heater are carefully designed for thermal isolation and easy fabrication.

The DML structure as shown in Fig. 1 does not have a passive waveguide because of adopting an all-active structure. The passive waveguide typically has been fabricated by butt-coupling process via etch and regrowth steps. However, the interface between active and passive waveguide may cause an internal reflection that can disturb the operation characteristics of the DFB LDs [23]. Therefore, the all-active structure provides us with easy fabrication steps and stable operations being free of the internal reflection at the interface between passive and active waveguides.

#113331 - $15.00 USD Received 24 Jun 2009; revised 7 Jul 2009; accepted 7 Jul 2009; published 24 Jul 2009

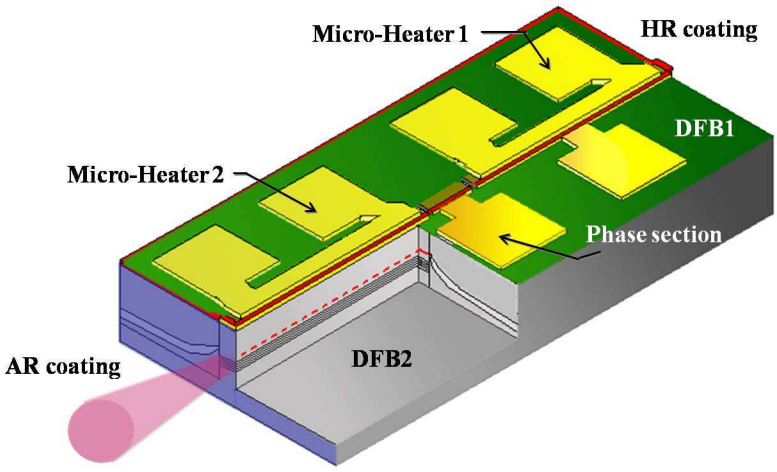

Fig. 1. Device structure of the dual-mode laser diode (DML)

We firstly grew seven strain-compensated quantum wells for the active layer and an InGaAs absorption layer on the active layer using metal organic chemical vapor deposition (MOCVD). The grating was patterned by using a typical holographic method on the entire region of the wafer. Following the pattern transfer onto a 30-nm-thick SiN_x layer, the InGaAs loss-coupled grating was formed by wet etching with a $HBr:HNO_3:H_2O$ solution. (The grating is not formed in the phase section but only in the DFB sections.) After the grating fabrication and the delineation of the active layer, the conventional planar buried heterostructure (PBH) has been realized via the regrowth of pnp current blocking layer and p-cladding layer [17]. The electrical isolation between the phase and DFB sections was achieved by deep etching. The etch depth was carefully chosen considering the trade-off between internal reflection and electrical isolation. After finishing the whole device processing for the p-side, we deposited a SiN_x layer followed by Cr/Au layers for the μ-heater fabrication. Finally, a high-reflection (HR) coating was applied to the facet of the DFB1 section as shown in Fig. 1 in order to compensate for the absorption and reflection losses in the phase and DFB2 sections, respectively.

3. Experimental results

Figure 2 shows the wavelength tuning characteristics of the single DFB LD. By fitting the optical spectrum below the threshold, we extracted the coupling coefficient, κL, of this DFB LD [24]. The extracted κL is 2.01-0.42j for a single 400-μm long DFB LD equipped with μ-heater. We also investigated the heater performance in case of a single DFB LD. By applying the current of 32 mA to the heater, the wavelength tuning of 3.4 nm is achieved. This corresponds to the heater efficiency of 17 nm/W. We believe that this high wavelength tuning efficiency is a result from the high heater resistivity of 196 Ω due to thin Au layer (~100 nm). The side-mode suppression ratio (SMSR) is maintained over 30 dB through the whole tuning range.

#113331 - $15.00 USD Received 24 Jun 2009; revised 7 Jul 2009; accepted 7 Jul 2009; published 24 Jul 2009

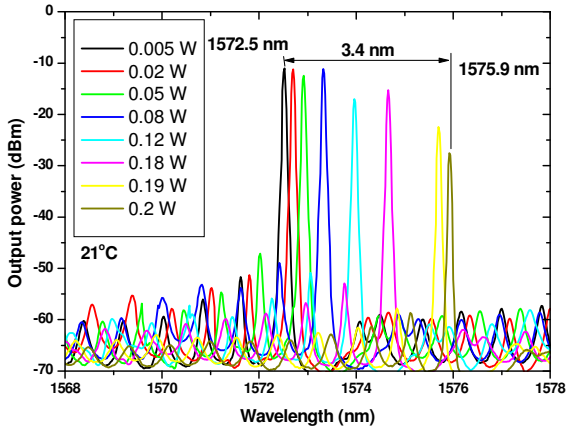

Fig. 2. Lasing spectra of the loss-coupled DFB laser with a length of 400 μm with varying the input μ-heater power.

In Fig. 2, the output power from the DFB LD decreases as the heater power increases. This phenomenon may originate from the fact that the gain peak moves toward longer wavelength faster than the lasing wavelength with increasing the heating current. In order to analyze the origin of the power degradation, a Fabry-Perot LD with μ-heater is fabricated and the gain spectra are measured with increasing the heating current using the Hakki-Paoli method, as shown in Fig. 3 [25].

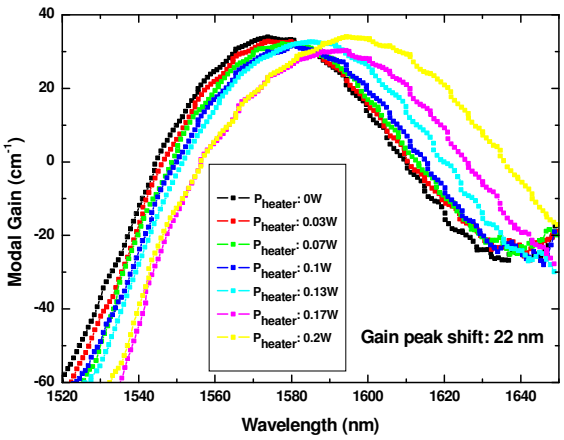

Fig. 3. Gain peak shift of a FP-LD as a function of the operation current of the μ-heater. The FP-LD has the same device structure with the μ-heater integrated DFB LD except grating layer.

The gain peak shifts to the longer wavelength as much as 22 nm showing the good performance of our μ-heater as one can see in Fig. 3. In order to estimate the temperature change of the active layer, we measured the gain spectra as increasing the LD mount temperature without μ-heater operations and compared the two gain-spectrum-shift data. The obtained temperature change of the active layer exceeds 50 °C at the μ-heater power of 0.2

#113331 - $15.00 USD Received 24 Jun 2009; revised 7 Jul 2009; accepted 7 Jul 2009; published 24 Jul 2009

W. Because the Bragg wavelength shift by thermal index variation is smaller than the gain peak shift of the active layer, the gain peak wavelength of the active layer should be located in shorter wavelength side than the Bragg wavelength to increase the tuning range.

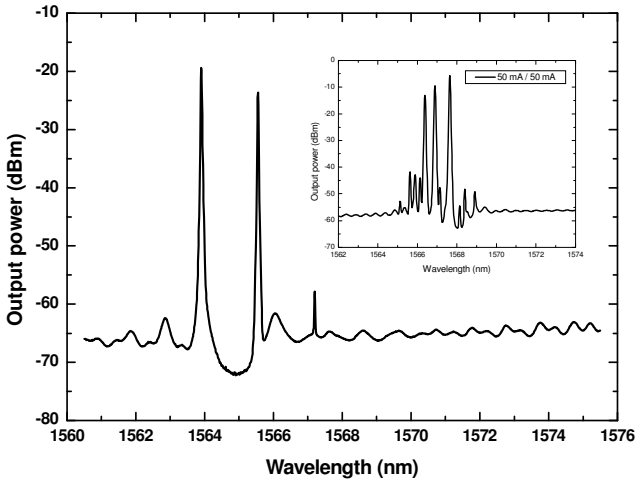

Fig. 4. Dual mode lasing spectrum of a HR/AR coated DML when a reverse bias is applied to the phase section. The operation current is 50 mA for each DFB section and the reverse bias is –0.3 V for the phase section. Inset shows the lasing spectrum when a forward bias is applied to the phase section. As increasing the reverse bias of the phase section, the optical loss is increased and the lasing of the complex compound-cavity modes is effectively suppressed.

The lasing spectrum of the fabricated DML measured with a reverse bias applied to the phase section is shown in Fig. 4. The SMSR and the initial wavelength difference are 34.4 dB and 1.7 nm, respectively. The inset of Fig. 4 shows the lasing spectrum of the DML when a forward bias is applied to the phase section. With the forward bias to the phase section, several compound-cavity modes in the DML occur as shown in the inset of Fig. 4 [19]. As the forward bias to the phase section increases, the optical absorption in the phase section decreases, so that many compound-cavity modes satisfy the lasing threshold condition. However, as the reverse bias into the phase section increases, the optical absorption is increased like an electro-absorption modulator. Therefore, the phase section under reverse bias acts like a saturable absorber in passively mode-locked lasers, which offers an optical correlation between the two main modes of the DML with increasing SMSR. Moreover, the reverse bias to the phase section enhances the thermal isolation between the two DFB sections, which helps independent tuning of each lasing mode.

The output power of the DFB1 is smaller than that of the DFB2 due to the optical loss through the phase section. Optical power balancing for efficient mode beating could be made by increasing the injection current of DFB1 section to compensate for the optical loss in the phase section. However, it can degrade the SMSR and cause the additional mode shift by the thermal effect. To solve the power balancing problem, as mentioned above, the HR coating was applied to the facet of DFB1 while the facet of DFB2 was anti-reflection (AR) coated.

#113331 - $15.00 USD Received 24 Jun 2009; revised 7 Jul 2009; accepted 7 Jul 2009; published 24 Jul 2009

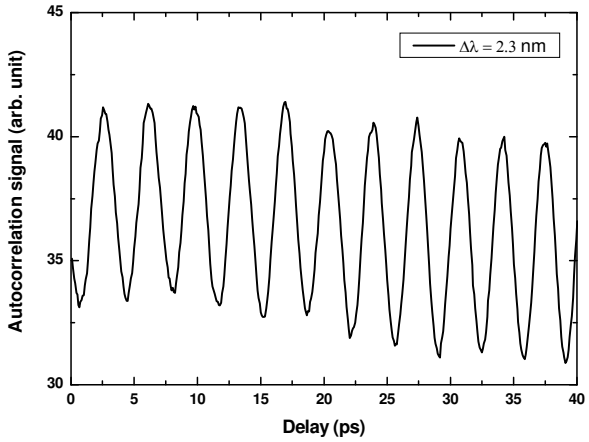

Fig. 5. Autocorrelation trace of DML. Wavelength difference between two modes is set to be 2.3 nm which is corresponding to 280 GHz.

Figure 5 shows an autocorrelation trace of the DML with 2.3 nm wavelength difference between two lasing modes. By turning on the μ-heater of DFB1 section operating at the longer wavelength side, the wavelength difference can be set to be 2.3 nm. The input heater power is 0.12 W in this case. The wavelength difference corresponds to the beat frequency of 280 GHz. The autocorrelation trace clearly shows the mode beating by the two lasing modes from the DML.

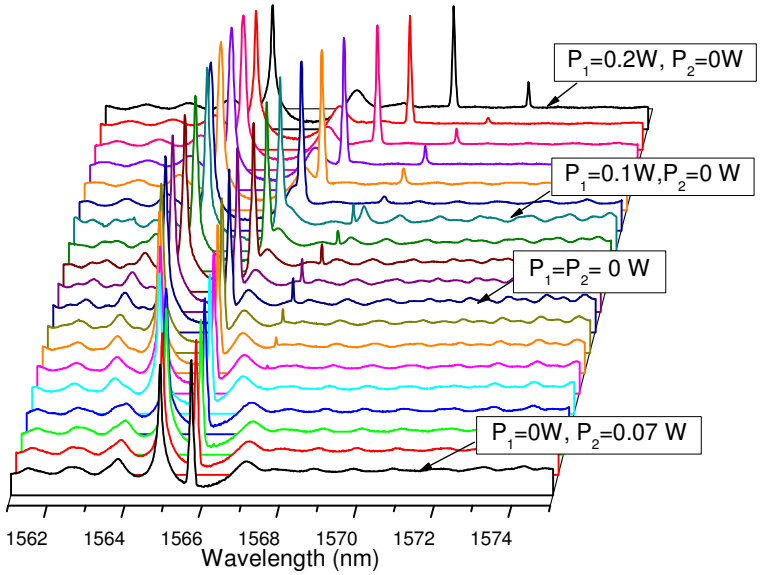

Fig. 6. Wavelength tuning characteristics of the HR/AR coated DML. The P_1 and P_2 represent the input μ-heater powers of the DFB1 and DFB2, respectively. The wavelength difference is tuned from 0.81 (0.10 THz) to 4.7 nm (0.57 THz) using μ-heaters.

Figure 6 shows the wavelength tuning characteristics of the HR/AR coated DML. The P_1 and P_2 in Fig. 6 represent the input μ-heater powers of the DFB1 and DFB2, respectively.

#113331 - $15.00 USD Received 24 Jun 2009; revised 7 Jul 2009; accepted 7 Jul 2009; published 24 Jul 2009

The spectrum of $P_1 = P_2 = 0$ W is same as that of Fig. 4. When P_2 increases up to 0.07 W, the DFB2 mode red-shifts by 0.9 nm with the DFB1 mode nearly unchanged. When P_1 increases up to 0.2 W, both the two modes red-shifts, of which the wavelength difference is increased up to 4.7 nm (0.57 THz). Therefore, the continuous tuning of wavelength difference from 0.81 nm to 4.7 nm is successfully demonstrated in our 3-section DFB laser. It is noticeable that the μ-heaters can control each mode independently as shown in Fig. 6. From this unique mode tuning characteristic of our DML, the tuning range could be easily extended by using the detuned grating for each DFB section. The achieved tuning range and SMSR (>30dB) shows the potential of our DML as a compact and cost effective optical beat source for the tunable CW THz generator.

The fabricated InGaAs photomixer (bowtie type) is shown in Fig. 7(a). For the fabrication of the InGaAs photomixers, 1.3MeV Fe^+ ions were irradiated onto a 0.7-μm-thick undoped InGaAs layer on a 2-inch InP wafer with the dose of $6x10^{14}$ cm^{-2}. And then, the wafer was annealed in a rapid thermal anneal (RTA) system at 500°C in a hydrogen environment [26]. After the RTA process, the active mesa was formed by wet etching for current isolation as shown in the SEM image in Fig. 7(a). Finally, the antenna and the interdigitated finger patterns were defined by using a stepper system and formed by the evaporation of Ti/Au metals. Two antenna structures were fabricated: one is a broad-band bowtie antenna and the other is a resonant dual dipole antenna with a peak at ~0.3 THz. The InGaAs photomixer chip was mounted onto a hyper-hemispherical Si lens for collimation and probe-tip biased. The optical beat signal from the DML was focused onto the photomixer gap by a tapered fiber after amplified by an erbium-doped fiber amplifier (EDFA). The amplified spontaneous emission from the EDFA was filtered out by using a band-pass filter with a bandwidth of 12 nm. Thanks to the monolithic DML, any mechanical alignment and/or polarization control between two beams were not needed. A cryogenic bolometer operating at 4.2 K was used to measure the power of THz wave emitted from the photomixers. In order to enhance the detection sensitivity, we used a lock-in amplifier with a square-wave pulse generator which modulated the photomixer bias.

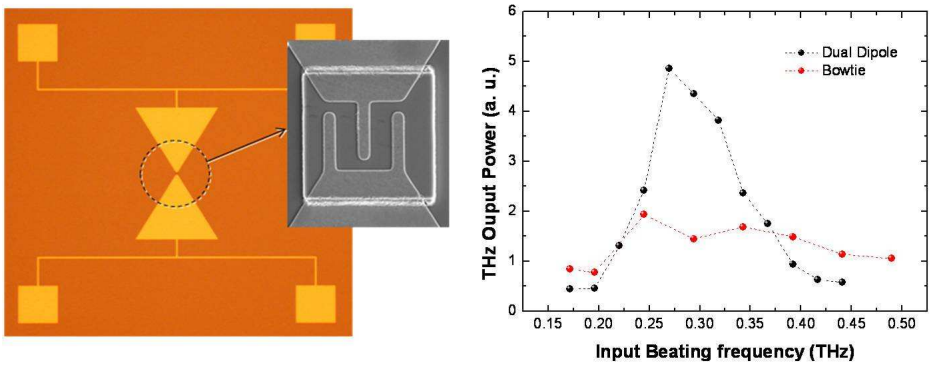

Fig. 7. (a) Microscope and SEM images of a fabricated Fe^+-implanted bowtie-type InGaAs photomixer, (b) Frequency tuning characteristic of THz emission from the InGaAs photomixers illuminated by our DML.

Figure 7(b) shows the continuous frequency tuning of the CW THz wave emitted from the fabricated Fe^+-implanted InGaAs photomixers illuminated by our DML. In Fig. 7(b), one can see the broad-band emission property of the bowtie antenna as well as the resonance property (~0.29 THz peak) of the dual dipole antenna as expected. The CW THz frequency is smoothly tuned from 0.17 to 0.49 THz as shown in Fig. 7(b). THz emissions above 0.49 THz

#113331 - $15.00 USD Received 24 Jun 2009; revised 7 Jul 2009; accepted 7 Jul 2009; published 24 Jul 2009

were limited by the gain bandwidth of the used EDFA. The number of interdigitated finger is 3. The dark resistance of the photomixer, the total optical input power, and the operation bias voltage of the photomixer were about 10 kΩ, 10 mW, and 2 V, respectively. The power decrease from the bowtie antenna below 0.25 THz range may not originate from the change of the total optical power or the power-balance breaking but from the input impedance irregularity of the bowtie antenna due to its finite size (800-μm diagonal). The detected THz output power from the dual-dipole antenna was estimated to be about 1 nW at 0.3 THz. This value is somewhat low compared to that of typical InGaAs-based photomixers [27], which might be due to the non-optimized photoconductive material properties such as the low dark resistance as well as the non-optimized photomixer structure and process. We believe that if material and process optimizations are achieved for the InGaAs photomixers, the THz output power would be greatly enhanced with our monolithic dual-mode laser as a tunable excitation source.

4. Conclusion

We demonstrated a wide wavelength tuning with high SMSR operation from a monolithic dual-mode semiconductor laser operating in the 1550 nm range for the application of the compact and tunable CW THz generation. The wavelengths of two modes could be independently tuned by adjusting currents in μ-heaters which were fabricated on the top of the each DFB section. The beat frequency from the dual-mode DFB laser was continuously tuned from 0.10 to 0.57 THz. The frequency tuning of the CW THz emission was also demonstrated using Fe^{+}-implanted InGaAs photomixers and our dual-mode laser as an excitation source. Thanks to the monolithic DML, any mechanical alignment and/or polarization control between two beams are not needed. The CW THz frequency was tuned from 0.17 to 0.49 THz. Our first result shows that the photomixing using the DML is very promising for the realization of compact and cost-effective tunable CW THz generator.

Acknowledgments

We thank Jang-Uk Shin, Sang-Pil Han and Yongsoon Baek for fruitful and useful discussions on the μ-heater fabrication and the device design.

#113331 - $15.00 USD Received 24 Jun 2009; revised 7 Jul 2009; accepted 7 Jul 2009; published 24 Jul 2009